Toward soil smart sensing in v4.0 agriculture: a new original single-shape design for a capacitive moisture and salinity sensor

Christophe Escriba, Julien Roux, Eli Gabriel Aviña Bravo, Jean-Yves Fourniols, M Contardo, Pascal Acco, Georges Soto-Romero

Toward soil smart sensing in v3.0 agriculture: a new original single-shape design for a capacitive moisture and salinity sensor

Julien Roux [1*], Christophe Escriba [1], Jean-Yves Fourniols [1], M. Contardo[2], Pascal Acco[1] and Georges Soto-Romero[1]

[1] Laboratory for Analysis and Architecture of Systems, LAAS, University of Toulouse, Toulouse F-31077, France; jroux@laas.fr; cescriba@laas.fr; fourniol@laas.fr
[2] TeleCommunications Services & Distribution, TCSD, Montauban, France; m.contardo@tcsd.fr
* Correspondence: jroux@laas.fr; Tel.: +33561336466

Abstract: To rationalise the amount of water needed to irrigate cultivated fields, modern agriculture imposes the need for better knowledge of the soil moisture content. In this context, since current technological solutions do not correspond to criteria of cost or use, this paper presents a design for a new original capacitive bi-functional sensor to measure soil moisture and salinity. In this paper, we outline all the stages of the design, from simulation to finished elements of the optimal design to deployment in the fields, taking into consideration the constraints of mechanical integration necessary for its industrialisation. Measurement electronics have been developed on the basis of an electric model of the sensor in order to obtain double measurement. Then, an on-site (field lot) measurement program was carried out to validate the good performance of the system in real time. Finally, this performance was matched with that of leading industrial sensors on the market. This work clearly demonstrates that, after deployment of the sensors, the overall system makes it possible to obtain a precise image of the hydric condition of cultivated soil, with the best response time.

Keywords: smart sensing; connected agriculture; capacitive bi-sensor; soil moisture and salinity.

1. Introduction

In modern and ecological agriculture, knowledge of the hydric condition of the soil has become an economic factor of major importance for the supply of water to crops. Accordingly, knowledge of moisture content and salinity is essential to the development of new irrigation systems. To meet this need, one of the most widely employed methods of measurement is the use of tensiometers [1]. Yet, this type of sensor has two main drawbacks: a response time of several hours, during which water is being supplied [2], as well as a phenomenon known as uncoupling [3]. These failings make it problematic to check the quantity of water supplied naturally (rain) or artificially (irrigation). Not only is it impossible to check the soil in real time, but, while these sensors are very sensitive, they often cease to work when the soil is too wet or too dry. In the latter event, it becomes necessary to reinstall sensors, which can be prejudicial to large farm operations.

Consequently, new capacitive measuring technology has been developed to modernise future agricultural installations. It is this capacitive measuring principle that we have selected to measure the level of moisture in the soil [4-6]. The main advantage of this type of sensor is that it possesses a response time of less than a minute, which gives it the ability to monitor the hydric condition of the soil in close to real time [7]. Existing solutions [8-10] include sensors based on a small-sized (<1 mm) detection cell), which limits the volume of soil that can be tested. On the other hand, their complex structures [11-13] do not make them easy to use and require some time, several months, to restructure the soil, which can be damaging to farmers.

Since alternative technologies to measure moisture do exist, let us examine the radiofrequency method [14-15]. This approach does not allow for a double measurement to evaluate soil salinity at the same time. To respond to this need, our solution exploits the capacitive properties of a sensor structure because it makes it possible to measure salinity as well as moisture [16-17]. Indeed, subject to a certain range of frequencies, soil capacity depends not only on moisture but also on its ionic composition [18]. Thus, by taking one moisture measurement followed by a measurement of moisture/salinity combined, the same sensor can obtain the two parameters.

To allow measurement on the scale of a large agricultural operation, multiplication of measurement points makes it possible to reach areas that are sufficiently representative of the soil's hydric condition. Several systems already have been created, but either their cost largely limits their deployment [19] or the existing system is technologically limited for large-scale use [20].

So, in response to these technological barriers, our innovation is based on the design of a new generation of affordable capacitive sensors that are compatible with the demands of deployment on a large scale. Section 2 presents an elementary design of the sensor and its optimization. Section 3 presents a modification of the shape factor of the electrodes to optimise measurement parameters. Section 4 describes the electric model of the sensor, while section 5 presents the design of on-board electronics for the associated measurement. Finally, section 6 outlines results of on-site performance tests on actual agricultural operations.

2. First approach and optimization

Initially, design of the transducer is based on the same principle as a condenser. The structure rests on two electrodes separated by a dielectric image of the soil. A cylindrical shape is preferred for this type of transducer to facilitate insertion into the soil. Copper electrodes are fixed to the cylinder as shown in Figure 1. Since the thickness of the electrodes is less than 1/10 mm, inter electrode $C_{electrodes}$ capacity is negligible.

Figure 1. Sensor shape, first design

For practical reasons and for reasons of mechanical solidity, a 40mm diameter is selected to demonstrate the feasibility of the initial transducer. Advantages are:

- ease of insertion into the soil. An auger with a standard diameter is used to make a pre-hole.
- soil is minimally de-structured around the sensor to avoid skewing measurements.

Electrodes and inter-electrodes must be large enough to ensure connectivity and minimise parasitic capacity between electrodes. To permit soil moisture detection of 10% with a planar surface capacity of 25pF, analytical calculations point to 40 mm electrodes spaced 10 mm apart.

First, the electrodes surface must be limited to lower the cost of fabrication. The objective is to reduce the diameter of the transducer while preserving the dimensions' homothetic relationship in order to minimally affect the ultimate capacity of the transducer. Work to re-dimension the

transducer makes it possible to obtain a 20mm diameter on electrodes with a width of 30mm, spaced 8mm apart. Figure 2 shows the evolution of capacities as a function of mass soil moisture for a diameter of 20mm as opposed to a diameter of 40mm.

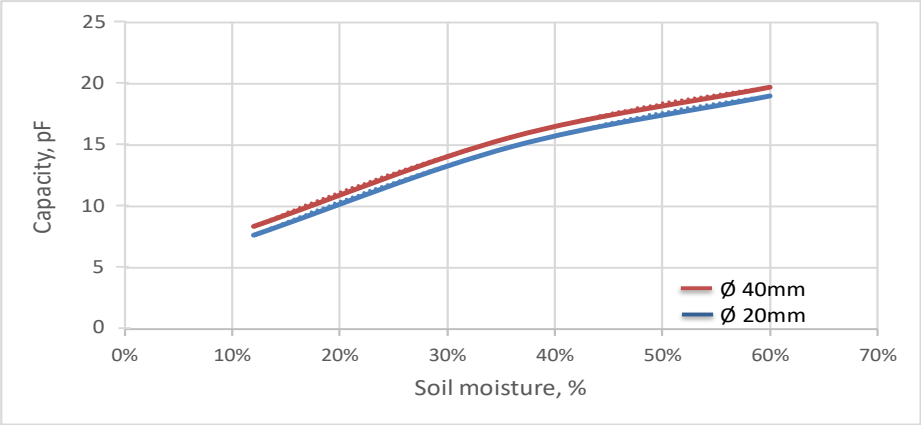

Figure 2. Cylindrical sensor capacity as a function of soil moisture

Curves show that the 20mm transducer has the same characteristics as the transducer with a 40mm diameter, with a sensitivity of 0.26pF.%$^{-1}$, a variation of 12.6pF subsequent to a 48% change in moisture.

Beyond the sensitivity of the sensor, it is necessary to estimate the volume of soil probed. In order to conduct this study, COMSOL modelling of the final elements was carried out. The volume of soil probed is quantified on the basis of the density of the electric field generated (Figure 3).

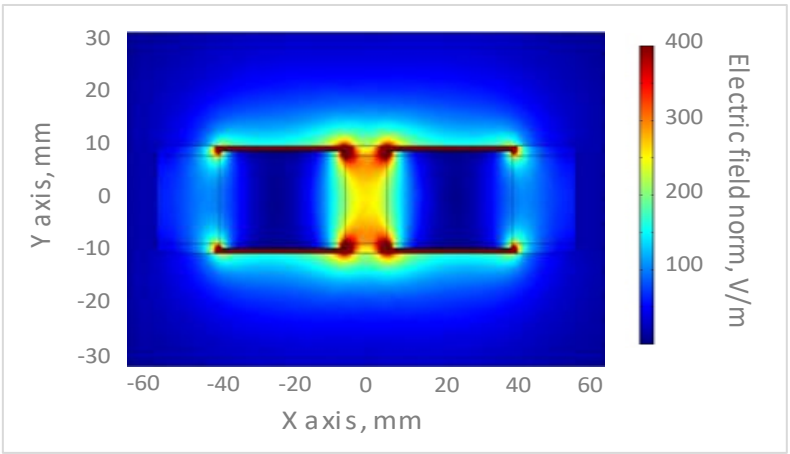

Figure 3. Density of electric field around cylindrical sensor

These simulation results show that a cylinder-shaped transducer with adapted electrodes (centred between (-20 ; 0) and (20 ; 0)) make it possible to observe a 50mm radius with an electric field density higher than 50V/m, which means that soil volume of about 1.32 litres, with a sensitivity of (0.26pF.%$^{-1}$) is needed in order to electronically probe a sufficient volume of soil. Yet the copper surface needed is relatively significant (15080 mm²), which raises the cost of the sensor. To optimise the dimensions of the transducer and thereby reduce the surface of the electrodes, Table 1 and

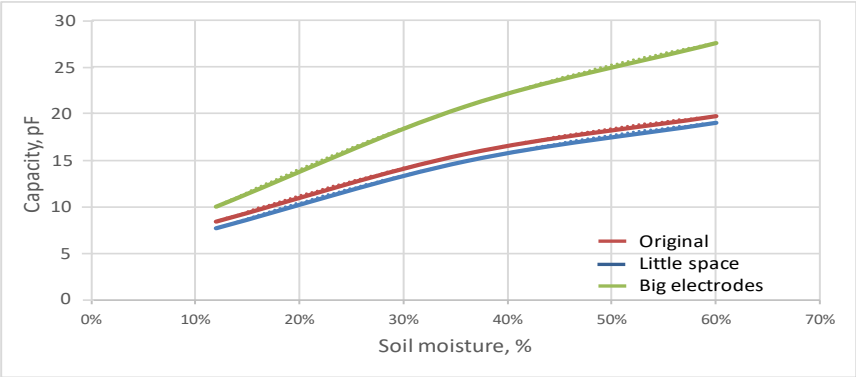

Figure 4 present results obtained:

Table 1. New electrode dimensions

Sensor	Diameter(mm)	Space between electrodes (mm)	Electrodes width (mm)	Electrodes surface (mm²)
Original	20	8	30	3769.91
Little space	20	5	30	3769.91
Big electrode	20	8	50	6283.19

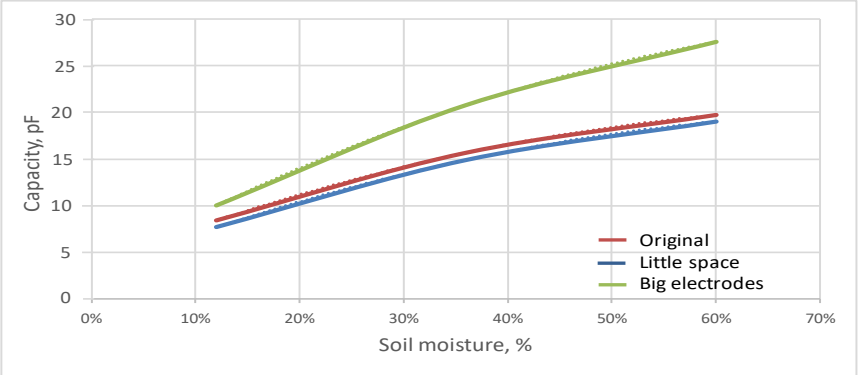

Figure 4. Capacity of different-sized electrodes as a function of moisture

Analysis of these results allows us to exploit them according to the "rules of electrode design":

- If we reduce inter-electrode space, capacity is higher but sensitivity is reduced by 11%, from an initial 0.265pF.%$^{-1}$ to 0.235pF.%$^{-1}$. This dimensional variation, therefore, is not viable.
- If we increase this space, capacity is too reduced and becomes impossible to exploit. It is preferable, therefore, to preserve a 10mm space between electrodes.
- If we increase electrode width, we increase capacity as well as the sensitivity of the sensitive element. In fact, we go from 0.265pF.%$^{-1}$ to 0.367pF.%$^{-1}$, an increase of 38%. However, we also increase electrode surface by 67% which raises their cost. The increase in sensitivity is not significant enough to justify the resulting cost increase.
- If we reduce the width of the electrodes, we reduce sensitivity but we gain on the cost.

At the end of this optimization work, Figure 5 presents the final shape of the sensor equipped with cylindrical electrodes.

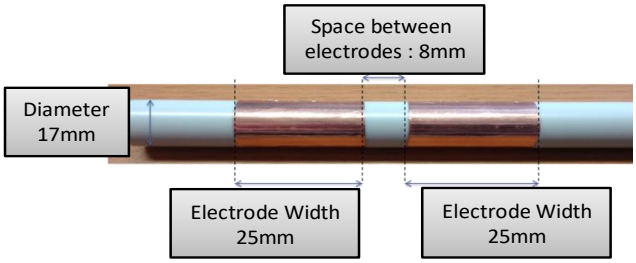

Figure 5. Optimized shape of first design

Even if the geometric dimensions are now optimized, we want to evaluate the influence of materials that are less costly than copper but preserve the same electric characteristics as copper. Identified materials are zinc, bronze, tin or their alloys. To conduct this study, partnership with the company Gilbert SA made it possible to produce several prototypes that we evaluated with an impedance analyser. It should be noted that, in the absence of the exact composition of alloys (for reasons of confidentiality), we have not carried out simulations with the final elements. Figure 6 shows measurement results obtained.

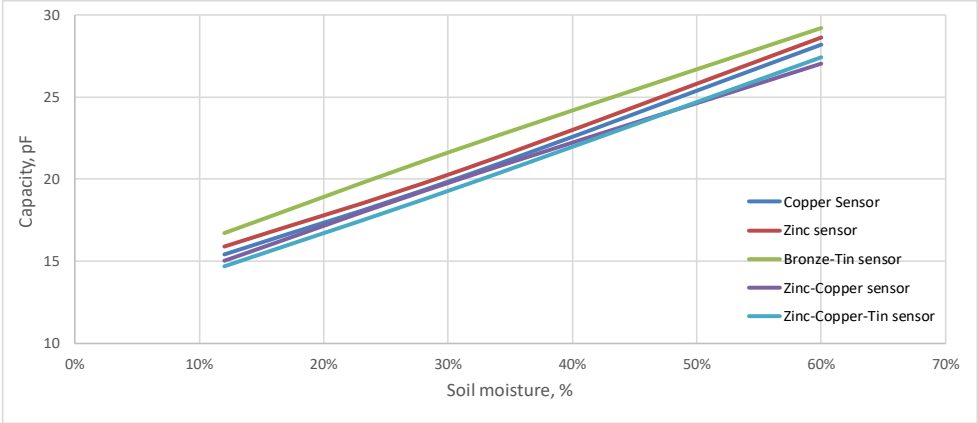

Figure 6. Capacity of different materials as a function of moisture

In Figure 6, we can see that copper, zinc and zinc-bronze-tin are suitable for the fabrication of electrodes. Nevertheless, in view of the steam fabrication process, copper, in spite of its higher cost, is the easiest to work with. It turns out, also, that the deposit process is more reliable for the fabrication of the electrodes. This explains why the metal electrodes of the transducer will be made of copper.

3. Toward new shapes with higher performance

With the cylindrical shape having been optimized from a geometric as well as a technological point of view, we now focus on a more complete optimization of the sensitivity and/or the volume of the probed soil. To do so, we propose to optimize the electrodes' shape factor.

3.1. New sensor shapes

The first parameter to optimise is sensitivity. Knowing that this parameter depends on the contact surface between the soil and the electrodes, it would seem to make sense to increase the contact surface. But in order to stay within initial cost limitations, the useful surface of the electrodes cannot be augmented. It must be distributed differently along the full length of the sensor. The

conceptual idea that we defend consists of spreading the electrodes longitudinally around the cylinder by shaping them into a double helix (Figure 7). This approach is directly inspired by the strands of DNA. The second parameter to optimise is the volume of soil probed. Knowing that this parameter depends on the paths of the transducer's field lines, optimization depends on augmenting these paths. In practice (Figure 8), we distribute the electrodes in the shape of branches on the periphery of the cylinder, placing them diametrically opposite each other.

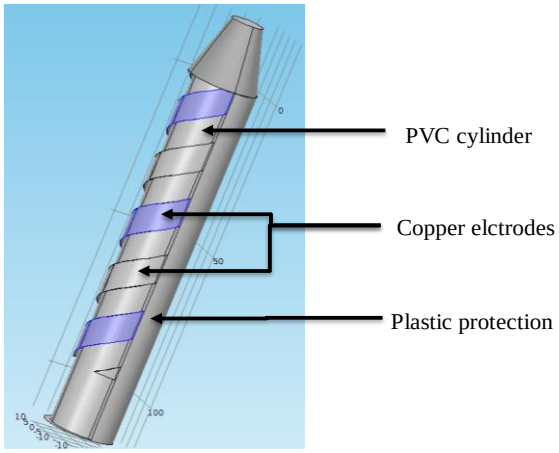

Figure 5. Sensor in the shape of a helicoid

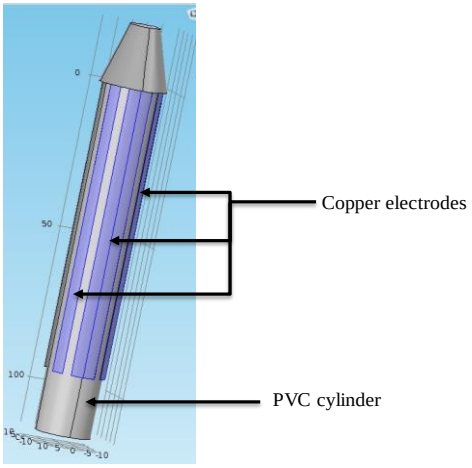

Figure 6. Sensor shape with "vertical ribbons"

The sensor with vertical ribbons (Figure 8) is equipped with two electrodes broken down into three ribbons, a main one in the centre and two 110mm lateral ones, for a total copper surface of 2670mm².

3.2. Determination of volume of soil probed

Simulation results confirm that the field created by the helicoidal sensor (Figure 7) is more uniform than that generated by the cylindrical shape. Assuming that the soil probed is traversed by an electric field of at least 50V/m, the helicoidal transducer probes a volume of 0.277L as opposed to 1.13L for the cylindrical shape. This decrease is subsequent to the division of the contact surface with a consequent reduction in the paths of these electric fields.

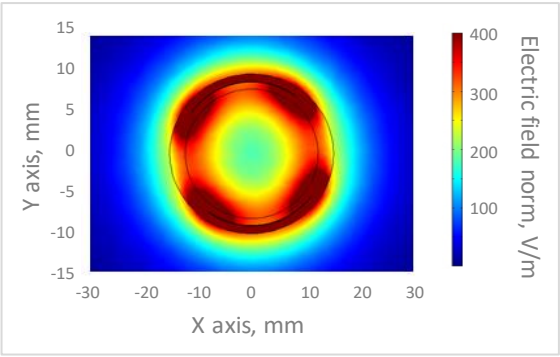

Figure 7. Electric field density around helicoidal sensor

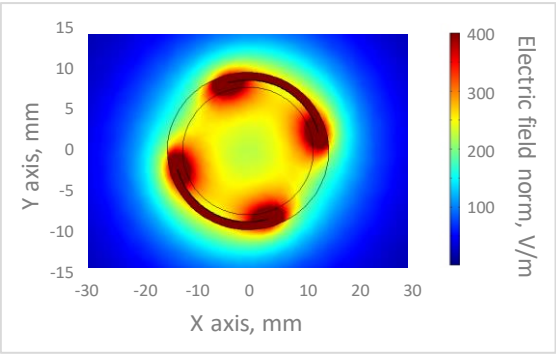

Figure 8. Electric field density around sensor with branches

As for the sensor with branches (Figure 8), its range of action is greater compared to the preceding shape. The volume of soil probed reached 1,737L, or six times more than with the

helicoidal framework, as well as 1.5 times more than the initial structure (cf. §2). This, therefore, is the new shape factor that permits soil testing on a larger scale.

To best illustrate the evolution in terms of electrical sensitivity, Figure 9 presents simulation results for the different sensors: cylindrical, double helix and with branches.

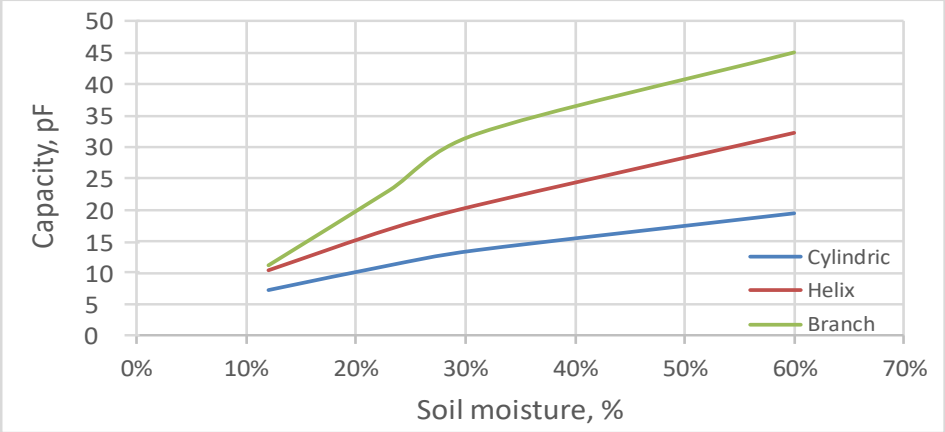

Figure 9. Capacity of different electrode shapes as a function of sensitivity to moisture

Sensitivity of the double helix shape is 67% higher, with a sensitivity of 0.4417pF.%$^{-1}$ compared with 0.265pF.%$^{-1}$ for the cylindrical sensor. Moreover, response linearity is much better. The transducer obtained is, therefore, more sensitive for an equivalent cost. For the sensor with branches, sensitivity also is improved -- by 0.7188pF.%$^{-1}$ or 171%. Nevertheless, the response obtained is not linear throughout the entire measurement. The graphic (Figure 9) shows two linear zones before and after 27% moisture in the soil. Electronic treatment will require two reading equations.

3.3. Choice of final shape

Table 2 reflects the characteristics of the three sensors studied. The overall performance of the sensor with branches stands out.

Table 2. Summary of sensor shape characteristics

Electrode Shape	Sensitivity (pF.%$^{-1}$)	Linear response	Probed soil (Litre)	Copper surface (mm^2)
Rings	0.265	Yes	1.32	2670.35
Double spiral	0.4417	Yes	0.277	2670.35
Branches	0.7188	No	1.737	2670.35

The sensor with branches is not only more sensitive, it also registers better soil volume. Clearly, its response is not linear, but this can be easily corrected with suitable measurement electronics. This shape is, therefore, the most suitable for our study. Nevertheless, in terms of industrialisation, this shape also is the costliest due to the discontinuous character of the electrodes. Manufacturers agree that the cost of fabrication is two times higher, compared to cylindrical or helicoidal shapes. Economic considerations therefore prevailed over performance in the choice of a helicoidal shape for the sensor.

3. Modelling the helicoidal-shaped sensor

4.1. Frequency analysis

Given the sensor's macroscopic capacitive behaviour as a function of moisture in the soil, this analysis (Figure 10) is necessary to identify the useful measurement frequency ranges.

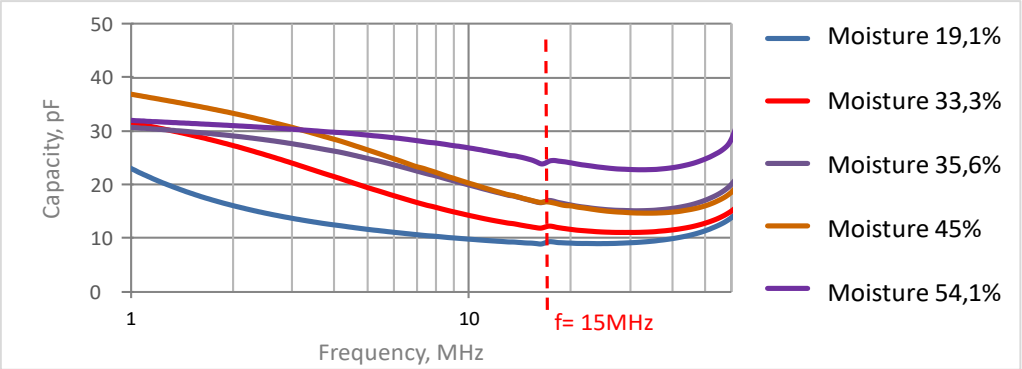

Figure 10. Sensor capacity as a function of the frequency

Figure 10 shows that:

- Capacity variations are inversely proportionate to moisture in the soil, which confirms theoretical functioning.
- As expected, capacity platforms at about 15MHz.
- Beyond this frequency, the inductive parasitic effect is no longer negligible. This demonstrates that beyond 15MHz, it becomes difficult to devise an exploitable electronic conditioner. Measurements are carried out below this frequency.

Since the greatest variances in capacity as a function of moisture fall between 1MHz and 15MHz, a working frequency close to 8MHz was chosen for the electronic conditioner.

Would it now be possible to endow the sensor with a second aptitude, so that it could measure salinity in the soil, depending on the possibility of finding a second frequency interval that would be sensitive to variations in soil salinity? To this end, we now install a measurement protocol analogous to the moisture measurement. Capacity is measured on a frequency ranging from kilohertz to around ten megahertz (Figure 11).

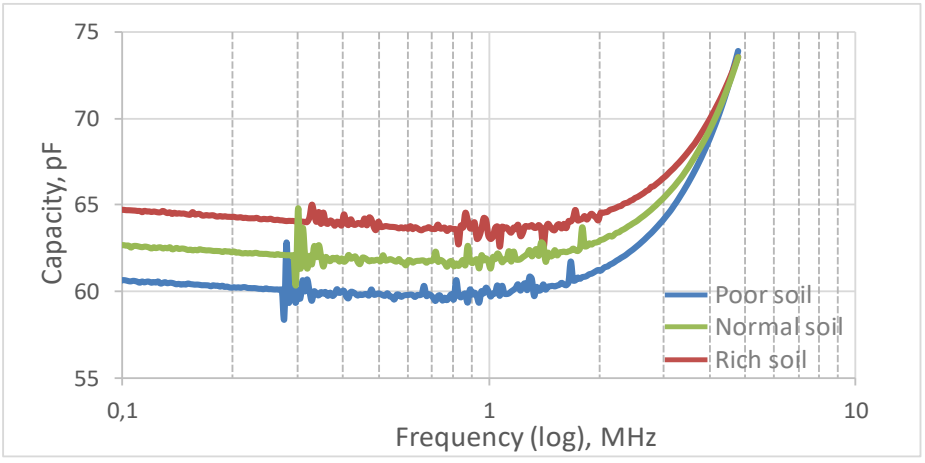

Figure 11. Sensor capacity as a function of the frequency for different levels of salinity

We observe that for frequencies higher than 4MHz, salinity has no influence on the capacity of the sensor. This means that the moisture measurement of the sensor is not influenced by the salinity of the soil, which makes the measurement independent. But below 4MHz, capacity increases with salinity. Yet, capacity does not depend on the measurement frequency as it does for the moisture

measurement. There is no preferred zone in this curve but perturbations are observed below 300kHz, which makes it necessary to avoid this zone. Measurement is, therefore, possible on all frequencies between 300kHz and 1MHz.

Figure 12 summarises all useable measurement frequencies.

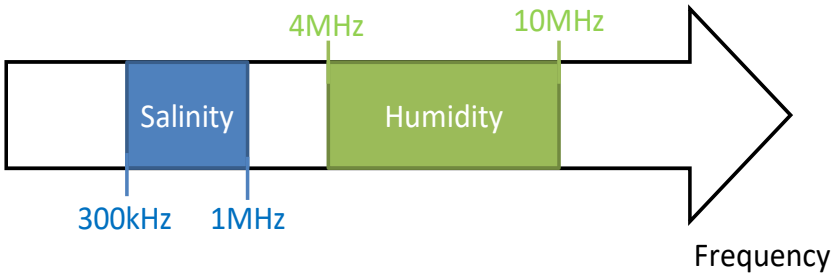

Figure 12. Measurement frequency zones for sensor

4.2. Integration effect

For reasons of mechanical protection, we have studied the effect of plastic coating on the sensor. Figure 13 provides a zoomed view of a cross-section of the sensor. This cross-section localises the coupling capacity between electrodes, coating and soil.

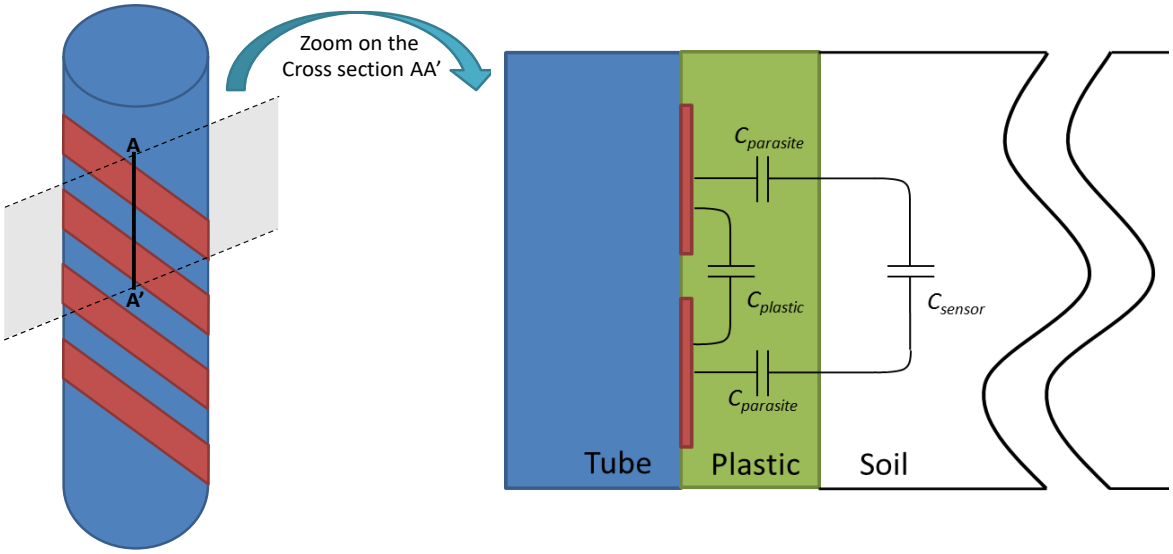

Figure 13. Effect of plastic protection on the sensor

Two supplementary pathways generated by the moulding can be observed:

- First, field lines close to the sensor only traverse the plastic and not the soil. This creates parasitic capacity where the dielectric is the plastic coating. Since this plastic is hermetic, its parameters are independent of moisture.
- Second, far-off field lines traverse the soil but also must traverse a layer of plastic coating which produces a series of parasitic capacity in addition to soil measurement capacity.

The transducer system may then be modelled as coated, according to the equivalent electrical diagram presented in Figure 14.

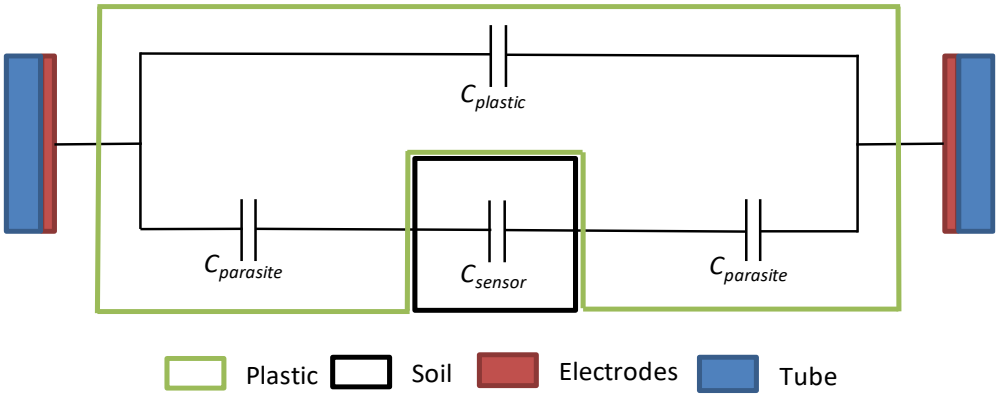

Figure 14. Model of the integration effect on the sensor

This model reveals two parasitic effects:

- Parallel $C_{plastic}$ capacity that adds to the $C_{humidity}$ measurement capacity.
- A $C_{humidity}$ measurement capacity that is altered by two parasitic capacities $C_{parasite}$. that end up in serial association with capacity $C_{parasite}/2$. This new measurement capacity turns out to be inferior to that of a non-integrated sensor.

Figure 15 shows the influence of the moulding on the sensitivity of the sensor.

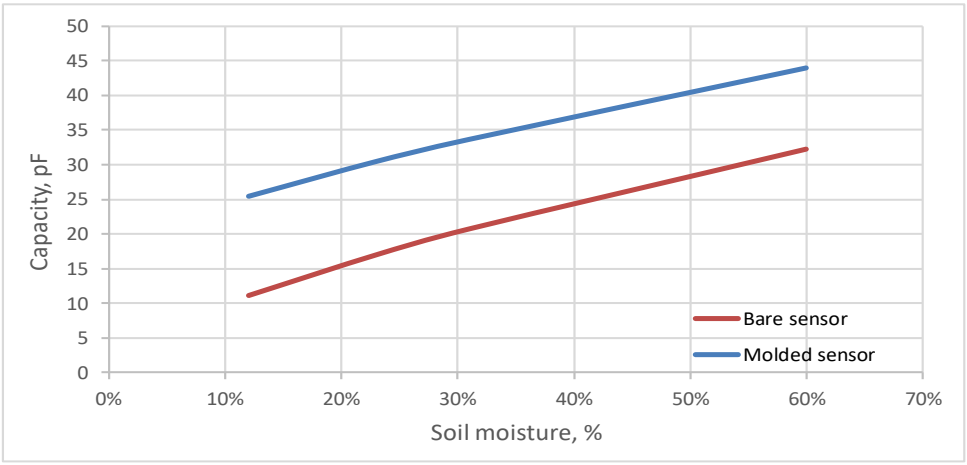

Figure 15. Moulded and unmoulded sensor sensitivity as a function of humidity

Two effects on the preceding model can be observed:

- The curve of the moulded transducer is superior in every way. It reflects the increase in C'_{hum0}, estimated at 14.7pF.
- Sensitivity is reduced by 12% with an estimated value of 0.3875pF.%$^{-1}$, a value always measurable by our system for a relative variation of 1% in moisture.

It should be remembered that the salinity measurement is affected on the same precise order of grandeur as that of moisture.

4.3. Equivalent electric models for sensors

Since sensor capacity is not perfect, we want to quantify the ESR, ESL and $C_{electrodes}$ imperfections of the equivalent model. The Equivalent Series Resistor (ESR) is the resistance that materialises contact between the two electrodes, with a measured value of ESR = 105mΩ. Equivalent Series Inductance (ESI) consists of the connecting wires that induce the inductive behaviour beyond 40MHz. Measurements show that ESL = 60µH. Finally, inter-electrode capacity is equal to $C_{electrodes}$ = 5.18fF. Figure 16 reflects this model.

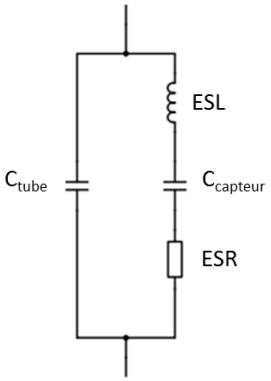

Figure 16. Electric model of the sensor

C_{sensor} capacity is associated with the type of measurement (moisture or salinity). Models equivalent to this capacity are shown in Figure 17 and Figure 18.

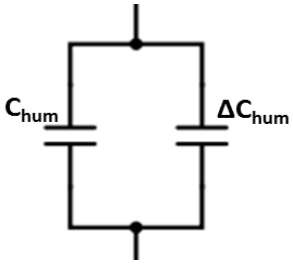

$$C_{sensor} = C_{moisture} = \Delta C_{moist} + C_{moist}$$

$$where \begin{cases} \Delta C_{moist}\ capacity\ variation\ with\ moisture \\ C_{moist}\ capacity\ for\ 0\%\ moisture \end{cases}$$

Figure 17. Final electric model for sensor as a function of moisture

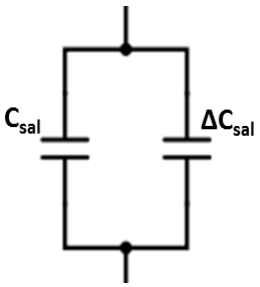

$$C_{sensor} = C_{salinity} = \Delta C_{sal} + C_{sal}$$

$$where \begin{cases} \Delta C_{sal}\ capacity\ variation\ with\ salinity \\ C_{sal}\ capacity\ for\ 0\%\ salinity \end{cases}$$

Figure 18. Final electric model for sensor as a function of salinity

To validate the transducer's electric model, a PSpice simulation makes it possible to check experimental results against the electric. Behavioural results are presented in Figure 21.

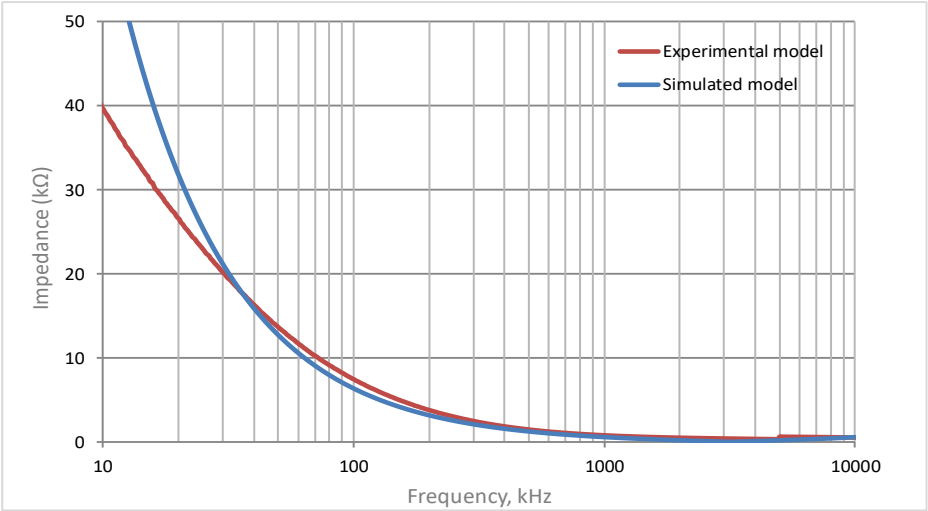

Figure 19. Validation of the sensor model by electric simulation

As of an impedance of 2.3kΩ at a frequency of *f*=35kHz, the curves are almost the same, then, as of *f*=400kHz, the curves are absolutely the same. Since useful frequency ranges are well above *f*=35kHz, the electric model for the sensor can be considered validated.

5. Measurement electronics

5.1. Architecture

The architecture that we have developed breaks down into two distinct parts (Figure 20). The first part is the front end. It permits the conversion of the sensor's capacity variations into one electric variation that is exploitable. Bearing in mind the frequency of readings and the low cost of the final system, the sensor is placed in a Colpitts oscillator to allow a capacity conversion frequency that depends on moisture or salinity. Since sensor must be able to perform two measurements, we decided to use two different oscillators set at f_{osc}= 8MHz for moisture and at f_{osc}=500kHz for salinity.

The back end, or second part of the architecture, delivers readings of the variations. To this end, the back end is structured around one microcontroller embedded with a frequency metre algorithm dedicated to double measurement of a frequency. To minimise the effect of temperature on the measurement, the microcontroller is equipped with a TCXO-type precision clock. To reduce the cost of the system, this microcontroller's frequency performances are voluntarily limited, which explains why the frequency is divided. Once this electronic treatment is accomplished, the back end proposes two types of complementary outlets, an analogue outlet that makes it possible to deliver voltage proportionate to moisture or to salinity with the aid of a CAN and a digital outlet that can be configured to establish a communications link with a standardised protocol (slave SPI).

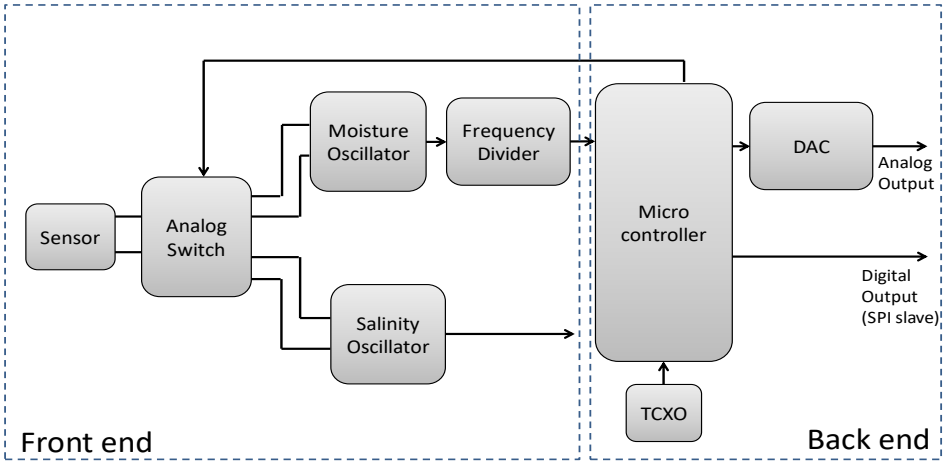

Figure 20. Functional diagram of measurement electronics

5.2. Material integration

In the process of industrial production of the sensor, the sensor tube will be manufactured according to an industrial procedure. The first stage consists of devising a cylindrical support tube. Then, the electrodes are produced according to photolithography and by electrochemical deposit of copper on a surface that has been made functional by a laser. Finally, a nickel/gold layer is deposited to protect the copper from oxidation. Figure 21 presents the finished sensor produced by this process.

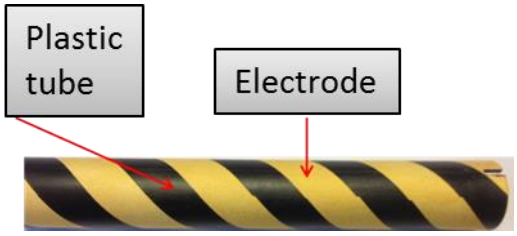

Figure 21. Shape of the industrially produced sensor

To control the thickness of the metallic deposit, measurement by optical profilometer is carried out. Readings of these measurements are presented in Figure 24.

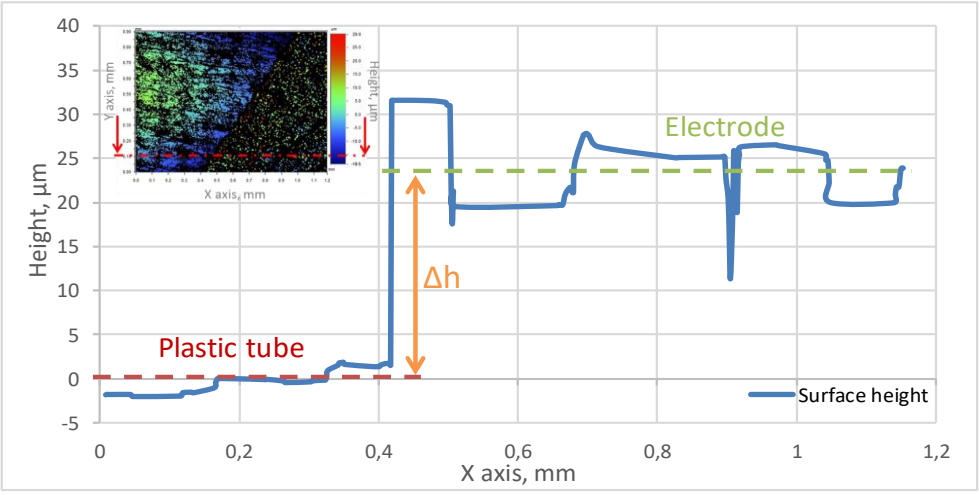

Figure 22. Electrode deposit profile

This figure shows:

- On the left of the graphic we can see the plastic tubing. It serves as reference to measure the height of the electrodes;
- On the right, there is the measurement of the average height of the metallic deposit: 24µm (20µm Cu, 4µm NiAu).

Since the sensor is to be inserted in the soil, it needs to be mechanically solid so that it is not damaged during its installation. As for the electronic board (Figure 25(a)), it is inserted in the sensor tube so that it forms a compact unit with no flexion points. To promote the mechanical longevity of the ensemble, recesses (Figure 25(b)) have been specifically sized.

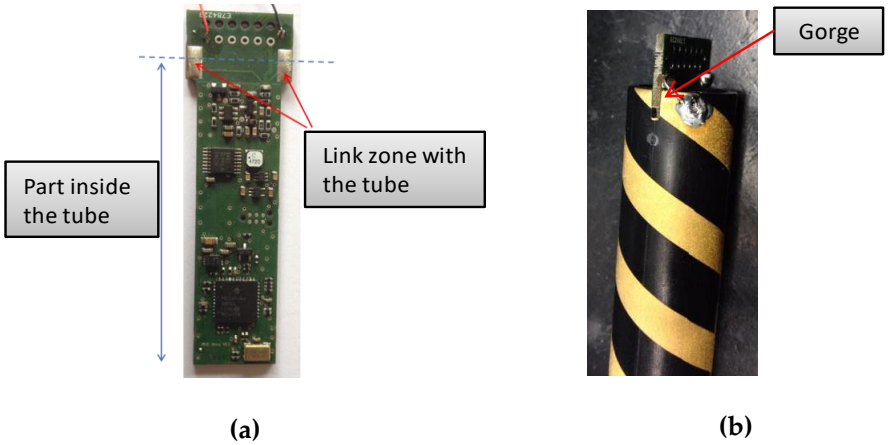

Figure 23. (a) Photo of the measurement electronic board; **(b)** Photo of the connection between the board and the sensor tube

To permit power supply and communication with the system, a protective shield is directly soldered onto specific landing pads. Finally, the sensor's water tightness is ensured by an injection of plastic into a mould. Figure 24 is a photo of the final sensor.

Figure 24. Photo of the industrially moulded sensor

5.3. From the sensor to the final user

With the aim of deploying the sensors in the cultivated fields, the architecture of the network is shown on Figure 27. It makes it possible to ensure the transmission of moisture and salinity measurement readings to the user. This infrastructure was developed with the support of the TCSD company. This company markets systems that collect data for agriculture (weather and soil).

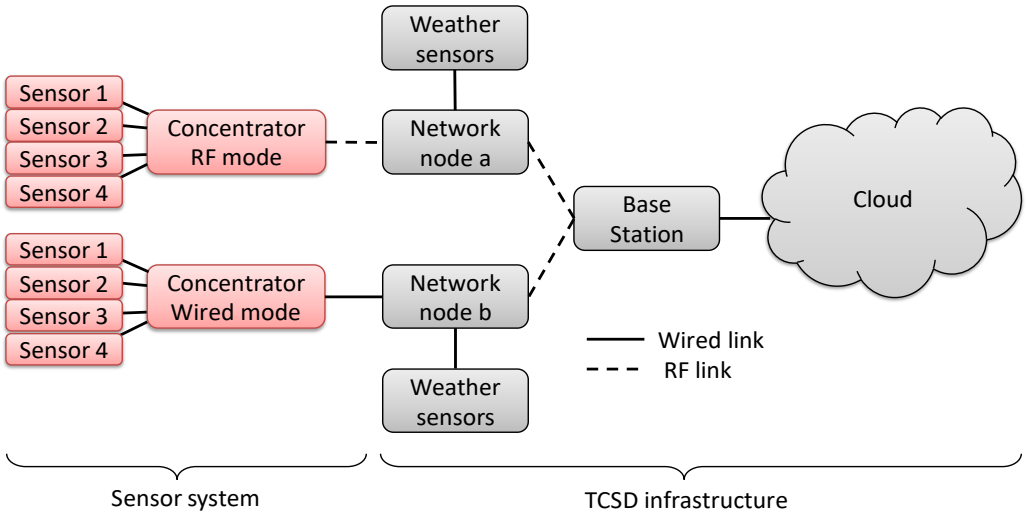

Figure 25. Architecture of sensor network

Figure 27 reflects the different stages of data collection:

- A concentrator supervises each sensor. Each concentrator can collect data from four sensors. It then communicates this data by a wire connection with an SDI-12 protocol, either by a radiofrequency link on the ISM 868MHz band to allow total control of the exchange protocol. Tests have demonstrated a radio range of 600m with a baud rate of 9600bits/s. Energy autonomy of the concentrator is provided by four AA batteries that last for an entire irrigation season (about 8 months). Figure 28 shows the electronic board.

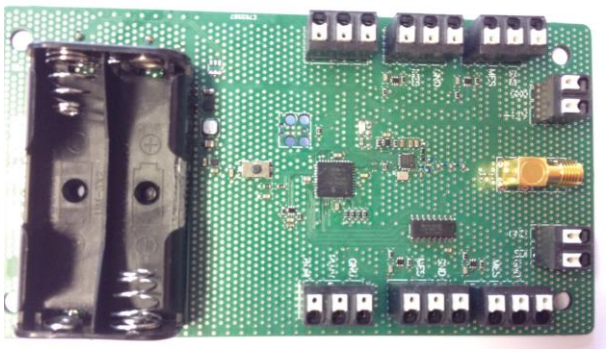

Figure 26. Photo of the electronic board produced

- Data then goes through the other network nodes that could be concentrators used in repeating mode or weather data collection points that also could serve as the bridge.

- Data finally arrive at a base station connected to the Internet, where information is stored on an on-line server. From then on, the user can consult the data by means of a web interface or mobile application.

6. Longitudinal moisture measurements

After the system is installed and deployed in cultivated and irrigated fields, moisture monitoring performance is compared to that of two major players in the market: Decagon and Sentek Technologies. As this work continues, the sensor that we have developed is called IRRIS for IRRIgation Ingénierie Systèmes.

Figure 27 presents measurement readings in an orchard that is cultivated all year round. Data from the IRRIS sensor shown on the graphic reflect three weeks of surveillance and are compared with that of the Decagon sensor.

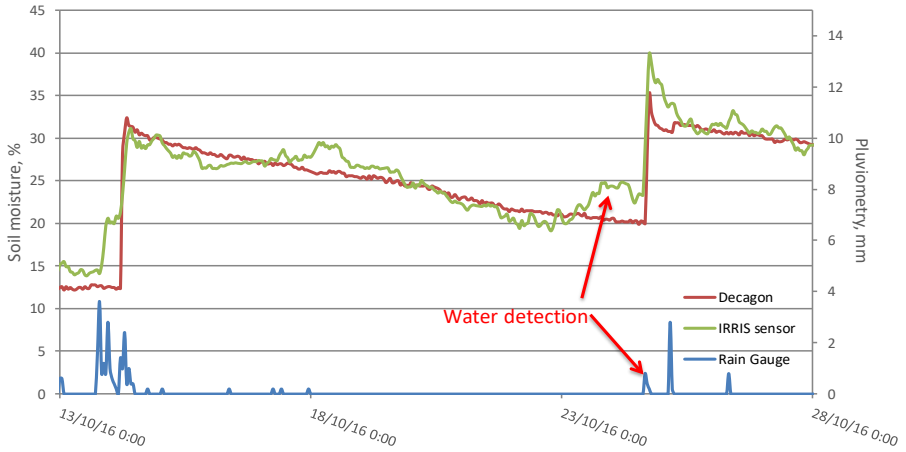

Figure 27. Results of a sensor in an orchard

The greater sensitivity of the IRRIS sensor is noticeable. As soon as the presence of water is detected by the IRRIS sensor, the moisture measurement increases, while the Decagon sensor does not detect this presence of water until after a few hours (red arrows). Detection, therefore, is better with the IRRIS sensor. The rising dynamic (+20%) and the descending dynamic (-2% per day) are identical for the two sensors, which validates the good performance of our sensor on this piece of agricultural land.

The second study addresses the surveillance of a corn field. Measurement readings reflect several days of continuous surveillance because of an installation made at the end of a cultivation cycle before the lot is harvested. Figure 28 presents results obtained.

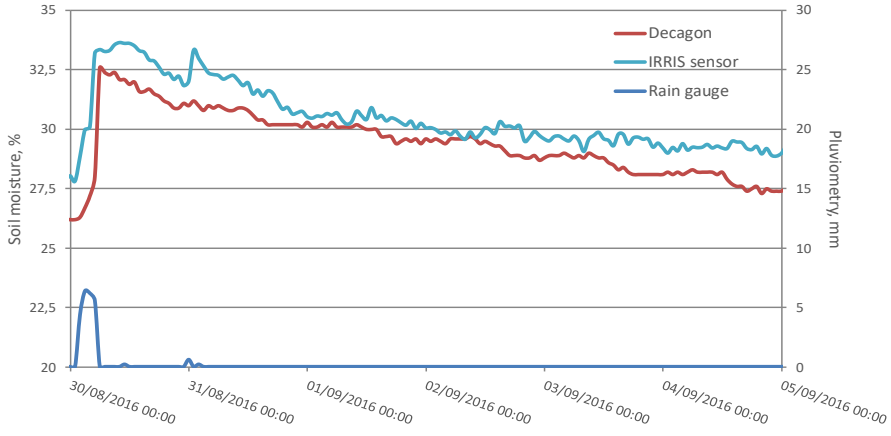

Figure 28. Sensor results in a corn field

This figure compares the dynamic and the response time of the IRRIS sensor compared with the Decagon sensor. In terms of reactivity, the IRRIS sensor reacts 30 minutes before the Decagon. With regard to dynamics, the moisture measurement rise due to the supply of water is identical for the two sensors (+7%). The descent dynamic is more rapid for the Decagon since it has been placed closer to the plants, and water is, therefore, more rapidly absorbed by the plants. These measurement readings testify to the good performance of the IRRIS sensor on this type of crop.

The last test is conducted with a Sentek sensor in another corn field. Figure 31 presents the results.

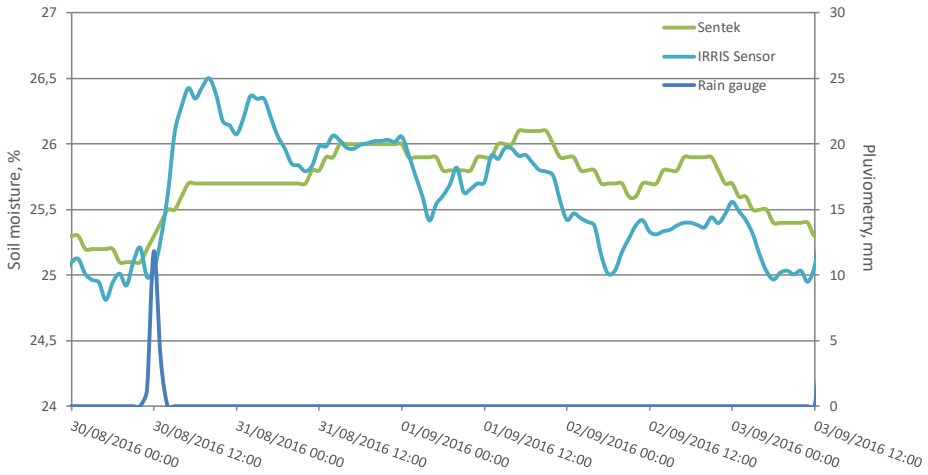

Figure 29. Sensor results compared with the Sentek sensor in a corn field

IRRIS sensor dynamics resemble those of the Sentek sensor. A measured rise in moisture after a supply of water followed by a slow descent on the scale may be clearly observed. What's more, this graphic shows the evapotranspiration effect. In fact, during a day/night cycle, it possible to observe a characteristic oscillation that displays this phenomenon. The IRRIS sensor also measures the phenomenon, which validates its performance.

To conclude on these tests, comparative response curves for the IRRIS sensors and the industrialised sensors attest to the superior performance of the IRRIS sensor. In this paper, we have shown that it is possible to detect small amounts of water more rapidly. This work clearly demonstrates the possibility of following these dynamic variations of moisture in the soil, when water is being supplied, as well as when the soil is drying out due to lack of water.

7. Conclusion

The sensor therefore is capable of measuring moisture and salinity in the soil for different types of crops. Thanks to its cylindrical shape, the sensor may be installed easily in the soil, and its different outlets (analogous wire, digital with or without wire) allow for a direct connection on most existing systems. Moreover, with a cost of fabrication estimated at less than 50€ per unit, its price makes it possible to multiply measuring points to better chart the hydric state of cultivated soil.

Acknowledgments

This work was done within the framework of the IRRIS project which is funded by the French Midi Pyrenees council and the French Ministry of Agriculture. Many thanks are due to TCSD (TelecommuniCation Service & Distribution) who lead the project and helped us to deploy our system into actual agricultural exploitation. We would thank Gilbert SA for their industrial support and their advices for the mechanical integration.

Author Contributions: C.E., J.Y.F and J.R. conceived, designed and performed the experiments; C.E. and J.R. analyzed the data; J.Y.F administrated the project; C.E. and J.R wrote the paper.

Funding: This research received no external funding.

Acknowledgments: We thank all the technical team of the LAAS-CNRS for all their support.

Conflicts of Interest: The authors declare no conflict of interest.

References

[1] B. Faybishenko, 'Tensiometer for shallow and deep measurements of water pressure in vadose zone and groundwater', *Soil Science*, vol. 165, no. 6, p. 473, Jun. 2000.

[2] M. Hayashi, G. van der Kamp, and D. L. Rudolph, 'Use of tensiometer response time to determine the hydraulic conductivity of unsaturated soil', *Soil Science*, vol. 162, no. 8, p. 566, Aug. 1997.

[3] C. M. Trotter, 'Errors in reading tensiometer vacua with pressure transducers', *Soil Science*, vol. 138, no. 4, p. 314, Oct. 1984.

[4] Z. Gao, Y. Zhu, C. Liu, H. Qian, W. Cao, and J. Ni, 'Design and Test of a Soil Profile Moisture Sensor Based on Sensitive Soil Layers', *Sensors*, vol. 18, no. 5, p. 1648, May 2018.

[5] T. J. Dean, J. P. Bell, and A. J. B. Baty, 'Soil moisture measurement by an improved capacitance technique, Part I. Sensor design and performance', *Journal of Hydrology*, vol. 93, no. 1–2, pp. 67–78, Aug. 1987.

[6] H. O. Buckman and N. C. Brady, 'The Nature and Properties of Soils', *Soil Science*, vol. 90, no. 3, 1960.

[7] F. Frasca, A. Caratelli, and A. M. Siani, 'The capability of capacitive sensors in the monitoring relative humidity in hypogeum environments', *IOP Conf. Ser.: Mater. Sci. Eng.*, vol. 364, no. 1, p. 012093, 2018.

[8] M. Chakraborty, A. Kalita, and K. Biswas, 'PMMA-Coated Capacitive Type Soil Moisture Sensor: Design, Fabrication, and Testing', *IEEE Transactions on Instrumentation and Measurement*, pp. 1–8, 2018.

[9] H. Kalita, V. S. Palaparthy, M. S. Baghini, and M. Aslam, 'Graphene quantum dot soil moisture sensor', *Sensors and Actuators B: Chemical*, vol. 233, pp. 582–590, Oct. 2016.

[10] V. S. Palaparthy, H. Kalita, S. G. Surya, M. S. Baghini, and M. Aslam, 'Graphene oxide based soil moisture microsensor for in situ agriculture applications', *Sensors and Actuators B: Chemical*, vol. 273, pp. 1660–1669, Nov. 2018.

[11] J. Boudaden *et al.*, 'Polyimide-Based Capacitive Humidity Sensor', *Sensors*, vol. 18, no. 5, p. 1516, May 2018.

[12] D. Xiao, J. Feng, N. Wang, X. Luo, and Y. Hu, 'Integrated soil moisture and water depth sensor for paddy fields', *Computers and Electronics in Agriculture*, vol. 98, pp. 214–221, Oct. 2013.

[13] P. C. Dias *et al.*, 'Autonomous soil moisture sensor based on nanostructured thermosensitive resistors powered by an integrated thermoelectric generator', *Sensors and Actuators A: Physical*, vol. 239, pp. 1–7, Mar. 2016.

[14] S. Pichorim, N. Gomes, and J. Batchelor, 'Two Solutions of Soil Moisture Sensing with RFID for Landslide Monitoring', *Sensors*, vol. 18, no. 2, p. 452, Feb. 2018.

[15] M. Rezaei, E. Ebrahimi, S. Naseh, and M. Mohajerpour, 'A new 1.4-GHz soil moisture sensor', *Measurement*, vol. 45, no. 7, pp. 1723–1728, Aug. 2012.

[16] B. Aljoumani, J. A. Sànchez-Espigares, N. Cañameras, G. Wessolek, and R. Josa, 'Transfer Function and Time Series Outlier Analysis: Modelling Soil Salinity in Loamy Sand Soil by Including the Influences of Irrigation Management and Soil Temperature: Modelling soil salinity in loamy sand soil', *Irrigation and Drainage*, vol. 67, no. 2, pp. 282–294, Apr. 2018.

[17] J. Singh *et al.*, 'Performance assessment of factory and field calibrations for electromagnetic sensors in a loam soil', *Agricultural Water Management*, vol. 196, pp. 87–98, Jan. 2018.

[18] S. Visacro, R. Alipio, M. H. Murta Vale, and C. Pereira, 'The Response of Grounding Electrodes to Lightning Currents: The Effect of Frequency-Dependent Soil Resistivity and Permittivity', *IEEE Transactions on Electromagnetic Compatibility*, vol. 53, no. 2, pp. 401–406, May 2011.

[19] M. Boada, A. Lazaro, R. Villarino, and D. Girbau, 'Battery-Less Soil Moisture Measurement System Based on a NFC Device With Energy Harvesting Capability', *IEEE Sensors Journal*, vol. 18, no. 13, pp. 5541–5549, Jul. 2018.

[20] E. da Costa *et al.*, 'A Self-Powered and Autonomous Fringing Field Capacitive Sensor Integrated into a Micro Sprinkler Spinner to Measure Soil Water Content', *Sensors*, vol. 17, no. 3, p. 575, Mar. 2017.